Available online at www.sciencedirect.com
SCIENCE DIRECT®
Journal of Chromatography A, 1036 (2004) 61–72
JOURNAL OF CHROMATOGRAPHY A
www.elsevier.com/locate/chroma

# Effectiveness of the H-root method for determining adsorption isotherms of protein–salt systems in open micro-channels

Blanca H. Lapizco-Encinas [a,1], Neville G. Pinto [a,*]

[a] *Department of Chemical and Materials Engineering, P.O. Box 210012, Cincinnati, OH 45221-0012, USA*

**Abstract**

The application of the H-root method (HRM) for predicting isotherm data for protein–salt systems in open-channel chromatographs is presented. HRM mainly consists of performing a regression of the chromatographic response of a system in order to predict the isotherms of the solutes. The method is applicable to proteins with Type I (Langmuir) isotherms. HRM enables a quick determination of the effects of salt on protein isotherms, to facilitate the development of preparative separation protocols of trace proteins in open micro-channel systems. Two configurations were investigated: micro open parallel plate system (μOPPS) and micro open tubular system (μOTS). The effectiveness of HRM was evaluated by simulating the behavior of these open-channel systems with mass-transfer effects included. The influence of operating and geometrical parameters was determined with a detailed parametric study. It was found that HRM can give good estimates of the adsorption isotherms in both micro-channel systems. This is primarily attributed to efficient mass transfer, which ensured correspondence to the equilibrium assumption of HRM. In general, the μOTS was found to give more accurate predictions than the μOPPS. This is attributed to the smooth circular perimeter of flow. Nevertheless, the difference in accuracy is generally insignificant, and with the proper selection of operating conditions, both systems are well suited for HRM.


*Keywords:* H-root method; Adsorption isotherms; Protein–salt systems; Open parallel plate systems, micro; Open tubular systems, micro; Mathematical modelling

## 1. Introduction

Liquid chromatography (LC) has enormous potential for preparative purification of biological and chemical substances. During the past two decades there has been an extraordinary growth in the application of LC for protein purification [1–4]. Since large samples and/or high concentrations are used [1–6], accurate equilibrium isotherm data are essential given that the band profiles are controlled by the non-linear competitive equilibrium isotherms [5,7]. Knowledge of the adsorption isotherms is very valuable in predicting column loading capacity [6] and separation characteristics.

Isotherms can be determined by static or dynamic methods. Both methods require special care to eliminate errors arising from the equilibrium not being achieved when the measurement is made. Static methods are time-consuming [7]. Often single-solute isotherms are determined experimentally and the competitive isotherms are predicted using theoretical estimation methods, which offer only limited accuracy [8]. Multicomponent isotherm data for liquid–solid systems are traditionally generated by batch methods. The main disadvantages of this method are that it is extremely time consuming and expensive [1].

Alternatively, dynamic methods based on chromatography can be used for the prediction of isotherm data with the advantages of higher accuracy and speed [7]. Some of the methods are elution by characteristic points (ECP) [5], frontal analysis (FA) [9], method of mass balance [1], method of composition velocities (MCV), tracer-pulse [1], elution on a plateau [1], inverse method [10] and the H-root method (HRM) [1,10,11]. The advantages and disadvantages of these various methods have been discussed elsewhere [1,5,8,10–18]. Of particular interest to this work is the HRM method.

HRM was derived from the H-transformation theory (HTT) of chromatography [14]. HTT was developed to predict the chromatographic response of a system by using the

* Corresponding author. Tel.: +1-513-556-2771; fax: +1-513-556-3473.
*E-mail address:* neville.pinto@uc.edu (N.G. Pinto).
[1] Present address: Microfluidics Department, Sandia National Laboratories, 7011 East Avenue, MS 9951, Livermore, CA 94551-0969, USA.

0021-9673/$ – see front matter © 2003 Elsevier B.V. All rights reserved.
doi:10.1016/j.chroma.2003.10.120

Langmuir parameters of the analytes and the operating conditions. The HRM method mainly consists of performing a back-calculation of HTT; i.e. the response of the chromatographic system is used to predict the Langmuir parameters of the analytes. Some of the advantages of this method are that it does not require detailed chromatographic data, a simple detector response can be used to obtain the information needed for the HRM calculations. The application of HRM is simple and highly efficient chromatographic columns are not mandatory in order to produce accurate results. A limitation of this approach is that it assumes a priori that a Langmuir isotherm model is valid [1,5,8,11–16]. It is, therefore, imperative to follow the estimations of the Langmuir coefficients with probe non-linear chromatographic experiments to validate the original assumption. Further details about HRM can be found in the literature [1,11,12,14–16].

There are two chromatographic stationary phases that are of importance in preparative protein separations: particulate media and the activated surface of open micro-channel systems. HRM has previously been investigated for packed-bed systems [1,12]. Open micro-channel systems are particularly useful for preparative purification of trace biomolecules. Features include minimal dilution of trace samples, good mass transfer and minimal flow dispersion. Toward the development of efficient procedures for optimizing the separation of trace species, particularly proteins, in open micro-channel systems, it is useful to develop rapid methods for determining overloaded isotherms. HRM is promising in this regard, since the good kinetic characteristics of the open-channel system are in concordance with the equilibrium assumption of the model.

In this study, the utility of the HRM method has been evaluated for two different configurations of micro-channels: μOTS and μOPPS. The ability to predict isotherm data for a protein–salt system was studied. The effect of salt on protein equilibrium adsorption is important in two major modes of preparative chromatography: ion exchange and hydrophobic interaction systems. In both cases, it is important to determine how isotherms change with salt concentration. HRM provides a versatile theoretical framework for obtaining these data efficiently from chromatographic responses.

## 2. Theory

### 2.1. μOPPS model

A schematic representation of the μOPPS is shown in Fig. 1. It is assumed that the flow regime in this channel is laminar and fully developed with negligible end effects. For this case, Spangler's [19] velocity profile was adapted. Since the cross-section under consideration is not elliptical, the original expression was integrated over the cross-section and normalized to obtain the modified version in Eq. (1).

$$v_y = -\frac{12}{7} v_{\text{avg}} \left( \frac{b^2 + d^2}{b^2 d^2} \right) \left( \frac{(x^2 - b^2)(z^2 - d^2)}{(x^2 - b^2) + (z^2 - d^2)} \right) \quad (1)$$

Adsorption of the solute is assumed to take place on the surfaces defined by the depth and length dimensions (side surfaces) of the channel, while the surfaces defined by the width and the length (top and bottom surfaces) are assumed to be inactive. This choice is based on the experimental μOPPS developed earlier [20]; the top/bottom surfaces are inert, while the side surfaces are activated for ion-exchange. It is further assumed that the adsorption (or ion-exchange) step is instantaneous relative to the mass-transfer rate. The predominant mass-transfer resistance is in the liquid phase, since the surface is assumed to be non-porous and ideally two-dimensional. Upon injection, the sample is evenly distributed along the channel cross-section, and the fluid density is assumed constant. With these assumptions it can be

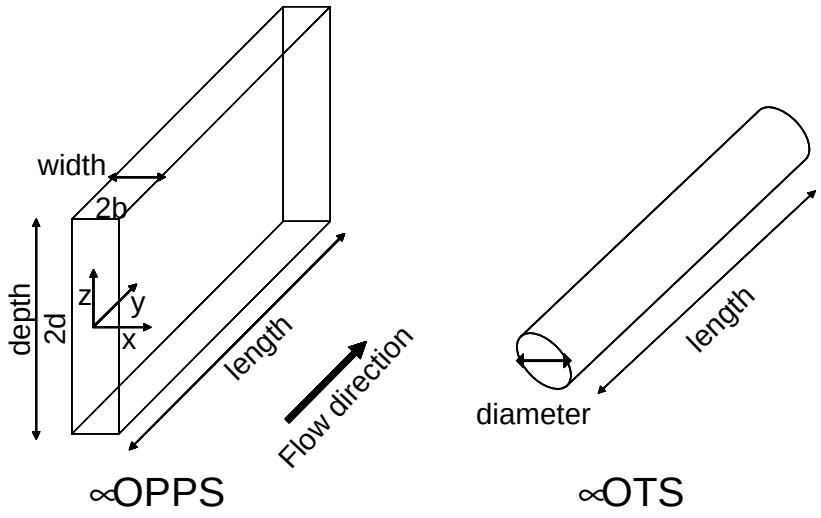


Fig. 1. Schematic representation of μOPPS and μOTS.

shown that a mass balance for a single solute in the channel is [21]:

$$\frac{\partial C_i}{\partial \tau} - \frac{12}{7}\frac{\partial C_i}{\partial Y}\left(\frac{b^2+d^2}{d^2}\right)\left(\frac{(X^2-1)(Z^2-1)}{(b^2/d^2)(X^2-1)+(Z^2-1)}\right) = \frac{1}{\theta_{X,i}}\frac{\partial^2 C_i}{\partial X^2} + \frac{1}{Pe_i}\frac{\partial^2 C_i}{\partial Y^2} + \frac{1}{\theta_{Z,i}}\frac{\partial^2 C_i}{\partial Z^2} \quad (2)$$

Initial and boundary conditions that apply to this equation in the elution and frontal modes of operation have been described elsewhere [22]. In order to solve Eq. (2), the numerical method of finite differences was applied. Forward difference was used for the first-order time derivative and central difference for all the spatial derivatives. In order to obtain a stable solution, the alternating direction implicit scheme was employed. This scheme divides each time interval between the number of spatial dimensions (in this case three dimensions): channel width, depth and length. Each spatial dimension is represented by a tridiagonal matrix of equations, which is solved using the LU-decomposition method (tridiagonal matrix method). The particular scheme used to solve Eq. (2) is the Peaceman Rachford algorithm and is described in detail elsewhere [21,22].

### 2.2. μOTS model

A schematic representation of the μOTS is shown in Fig. 1. The same assumptions used for the μOPPS are employed for the μOTS. With these assumptions, a mass balance for a solute in the μOTS is [21,22]:

$$\frac{\partial C_i}{\partial \tau} + 2(1-R^2)\frac{\partial C_i}{\partial Y} = \frac{1}{Pe_i}\frac{\partial^2 C_i}{\partial Y^2} + \frac{1}{\theta_{R,i}}\frac{1}{R}\frac{\partial C_i}{\partial R} + \frac{1}{\theta_{R,i}}\frac{\partial^2 C_i}{\partial R^2} \quad (3)$$

Eq. (3) was solved using the same numerical scheme that was used for Eq. (2).

### 2.3. Description of the HRM

HTT was developed by Helfferich and Klein [14]. It is used to predict the dynamic response of a fixed-bed column and has been extended to non-stoichiometric systems that obey the Langmuir isotherm:

$$q_i^* = \frac{V_{m_i} K_{m_i} C_i}{1+\sum_{j=1}^{nc} K_{m_j} C_j} = \frac{a_i C_i}{1+\sum_{j=1}^{nc} K_{m_j} C_j} \quad (4)$$

HRM derived from HTT, was first proposed by Chen et al. [1] and subsequently modified by Jen and Pinto [11]. HRM consists of two main parts: linear elution experiments to calculate the linear isotherm coefficient $a_i$ (Eq. (4)), and non-linear frontal experiments to calculate the competitive interference parameter $K_{m_i}$ (Eq. (4)). Only the breakthrough time of each front is necessary, which can be obtained directly from the detector response (Fig. 2). The kinetic effects that influence the shape of the peaks are not very significant in HRM, since the detailed frontal chromatogram is not needed. This is a significant advantage over FA and ECP methods, since in order to decrease the influence of kinetic effects for these methods, very efficient columns have to be used [8].

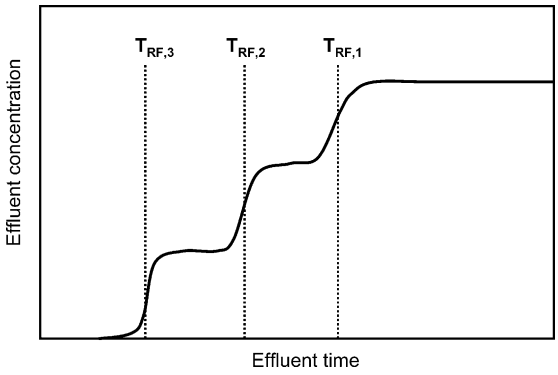


Fig. 2. Typical frontal detector response for a three-component mixture.

The μOPPS and μOTS are devices whose performance has a strong dependence on the width or diameter of the micro-channel. By using a very narrow micro-channel, it is possible to achieve a very efficient configuration, with reduced plate height values as low as 2 [21]. In the present work, an adaptation of HRM to the open geometries of the μOPPS and μOTS is presented. No attempt is made here to explain the basis of HTT or HRM. Details can be found in the literature [1,11,12,14–16,18].

### 2.4. HRM for open microcolumns

Since the equations in the literature describing chromatographic performance in the HRM framework are for traditional packed columns, it was necessary to adapt the equations for the open geometry of the μOPPS and μOTS. It can be shown that the concentration velocity in the μOPPS is [22]:

$$\left(\frac{\partial y}{\partial t}\right)_{C_i} = v_{C,i} = \frac{v_{avg}}{1+(1/b)(\partial q_i^*/\partial C_i)} \quad (5)$$

For the μOTS it is [22]:

$$\left(\frac{\partial y}{\partial t}\right)_{C_i} = v_{C,i} = \frac{v_{avg}}{1+(2/r_C)(\partial q_i^*/\partial C_i)} \quad (6)$$

In the linear region of the isotherm;

$$q_i^* = a_i C_i \quad (7)$$

Thus, the expressions for the concentration velocity for the μOPPS and μOTS in the linear regime simplify to:

$$\left(\frac{\partial y}{\partial t}\right)_{C_i} = v_{C,i\mathrm{OPPS}} = \frac{v_{avg}}{1+(a_i/b)} \quad (8)$$

$$\left(\frac{\partial y}{\partial t}\right)_{C_i} = v_{C,i_{\mathrm{OTS}}} = \frac{v_{avg}}{1+(2a_i/r_C)} \quad (9)$$

The linear elution experiments involve three steps: (1) equilibration of the column with a suitable eluent (salt solution); (2) injection of a short pulse of the mixture of solutes; and (3) development of the chromatogram. The retention time ($T_{R,i}$) of each component is used to calculate its linear isotherm coefficient $a_i$. For the μOPPS:

$$a_{i,\mathrm{OPPS}} = \left(\frac{v_{\mathrm{avg}}}{v_{\mathrm{C},i}} - 1\right) b = \left(\frac{T_{\mathrm{R},i}}{T_0} - 1\right) b \tag{10}$$

For the μOTS:

$$a_{i,\mathrm{OTS}} = \left(\frac{v_{\mathrm{avg}}}{v_{\mathrm{C},i}} - 1\right) b = \left(\frac{T_{\mathrm{R},i}}{T_0} - 1\right) \frac{r_{\mathrm{C}}}{2} \tag{11}$$

Non-linear frontal chromatography experiments are performed to obtain the competitive interference parameter $K_{m_i}$ for each component. The feed sample must be large enough for the two components to be eluted under non-linear conditions and interfere strongly. If the column is overloaded but the bands of the components are still separated, the determination of competitive isotherms is not possible [7]. The steps involved are: (1) equilibration of the column with the eluent (salt solution); (2) introduction of a step injection of the mixture; and (3) development of the frontal chromatogram to obtain the breakthrough time of each front. The breakthrough time of each front is then used to calculate the competitive interference coefficients ($K_{m_i}$) using the following equations [11,22]:

$$\sum_{i=1}^{n} \left(\frac{K_{m_i} CF_i}{(k_i/K_n) - 1}\right) - 1 = 0 \tag{12}$$

$$\sum_{i=1}^{n} \left(\frac{K_{m_i} CF_i}{(K_{j+1}/K_j)(k_i/k_{j+1}) - 1}\right) - 1 = 0$$
$$(1 \le j \le n-1) \tag{13}$$

where:

$$k_i = \frac{T_{\mathrm{R},i} - T_0}{T_0} = \phi a_i \tag{14}$$

$$K_i = \frac{T_{\mathrm{RF},i} - T_0}{T_0} = \frac{v_{\mathrm{avg}}}{v_{\mathrm{C},i}} - 1 \tag{15}$$

## 3. Numerical simulations

Simulations were performed in order to compare the capabilities of the μOPPS and μOTS for predicting isotherm data with HRM. The chromatographic responses of the μOPPS and μOTS were simulated with Eqs. (2) and (3), respectively. HRM is an equilibrium model. The μOPPS and μOTS simulators include mass-transfer effects to simulate real conditions. Therefore, the validity of using an equilibrium model to separate out thermodynamic properties from a chromatogram influenced by kinetics can be verified. In addition, the effects of column dimensions, and operating conditions were evaluated.

Table 1
Molecular properties for simulations

| Solute | $D$ (cm$^2$/s) | $M_r$ (g/mol) | $K_m$ (cm$^3$/μmol) | $a$ (cm) |
|---|---|---|---|---|
| NaCl | $2.0 \times 10^{-5}$ | 58.43 | 70.8 | $7.08 \times 10^{-3}$ |
| Conalbumin | $5.94 \times 10^{-7}$ | 80000 | 228.8 | $1.92 \times 10^{-2}$ |

Table 2
Operating conditions for the linear elution and non-linear frontal simulations

| Operating parameters | | | |
|---|---|---|---|
| Parameter | Value | Parameter | Value |
| $b$ or $r_C$ (μm) | 10–30 | $L$ (cm) | 2–20 |
| $d$ (μm) | 10–300 | $v_{avg}$ (cm/s) | 0.001 |
| Linear elution simulations | | Non-linear frontal simulations | |
| CF (μmol/cm$^3$) | 0.0001 | CF (μmol/cm$^3$) | 0.05 |
| VF (% of VC) | 1 | VF (% of VC) | 300 |

The protein–salt system selected was conalbumin (CON) and NaCl, adsorbing competitively on a polyethyleneimine coated, silica-based weak adsorbent. The experimental Langmuir parameters, diffusion coefficients and molecular weights used are summarized in Table 1. Diffusion coefficients and molecular weights were obtained from Tyn and Gusek [23]. The equilibrium adsorption of conalbumin was measured on the ion exchanger PAE-1000 (10 μm) at 30 °C from a solution at pH 7. The isotherm was obtained from batch measurements as has been described by Chandavarkar and Pinto [24]. The ranges for operating parameters used for chromatographic simulations are shown in Table 2, unless otherwise stated; the values of *CF* and *VF* were the same for protein and salt. The parameter $a_i$ was calculated from the chromatograms using Eqs. (10) and (11) for the μOPPS and μOTS, respectively. The interference coefficient ($K_{m_i}$) was calculated using Eqs. (12) and (13). The percentage deviation was calculated as follows:

$$\text{deviation (\%)} = \left(\frac{\text{experimental} - \text{predicted}}{\text{experimental}}\right) 100 \tag{16}$$

For the μOPPS, simulations were performed for the effects of α, $Pe_i$ and $\theta_{X,i}$, where:

$$\alpha = \frac{\theta_Z}{\theta_X} = \left(\frac{d}{b}\right)^2 \tag{17}$$

For the μOTS, the parameters varied were $Pe_i$ and $\theta_{R,i}$.

## 4. Results and Discussion

### 4.1. Prediction of linear isotherm coefficients ($a_i$)

The determination of the linear isotherm coefficient for the protein as a function of salt concentration by HRM, requires experimentally obtaining isocratic protein elution peaks at a suitable number of salt concentrations over the range of interest. One factor that can be expected to affect

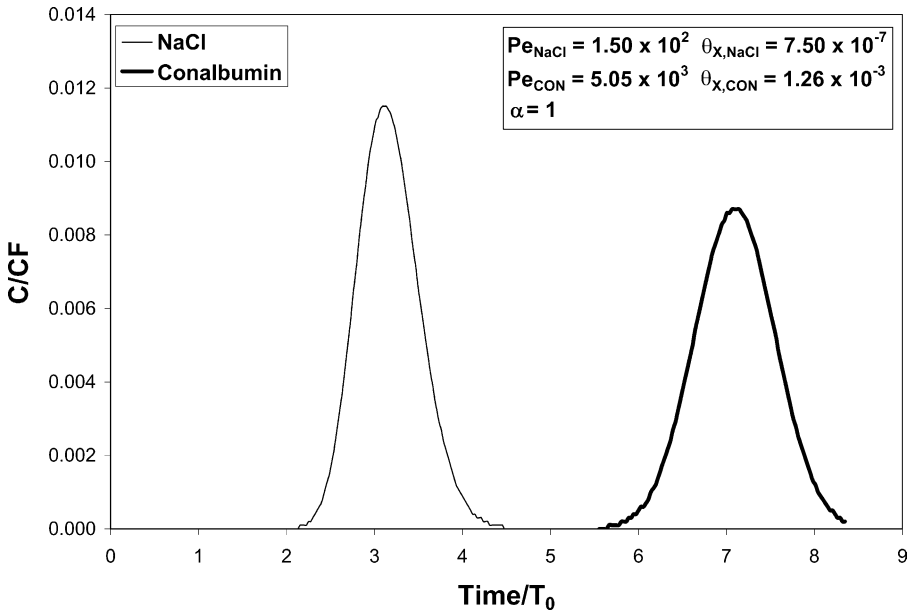


Fig. 3. Typical simulation results for linear elution.

the accuracy of the estimation of this coefficient from the chromatograms is the Peclet number (*Pe*). Since HRM is based on the equilibrium assumption, the method is expected to be less effective for a system with a larger *Pe*. Shown in Fig. 3 is a typical simulation used for the calculation of the linear isotherm coefficient ($a_i$) with HRM. The particular case is for the protein eluting at zero salt concentration from the μOPPS. Also shown, for completeness, is the relative retention of the salt on the adsorbent selected. Fig. 4 shows the influence of *Pe* on the linear isotherm prediction from $a_{CON}$ values measured using the μOPPS. As expected, an increase in *Pe* leads to an increase in the deviation in the prediction of $a_i$; i.e. a greater deviation of the predicted isotherm from the experimental isotherm. The deviations range from 4 to 6% for conalbumin. These results imply that mass transfer from the liquid to the channel surface has an influence on the accuracy of the predictions. This effect is, however, small. In Fig. 4, a change in the *Pe* of an order of magnitude changes the accuracy by only a few percent.

The influence of liquid-phase mass transfer is evident in the results for the effect of $\theta_X$. The channel width is the characteristic length of diffusion for adsorption, since ad-

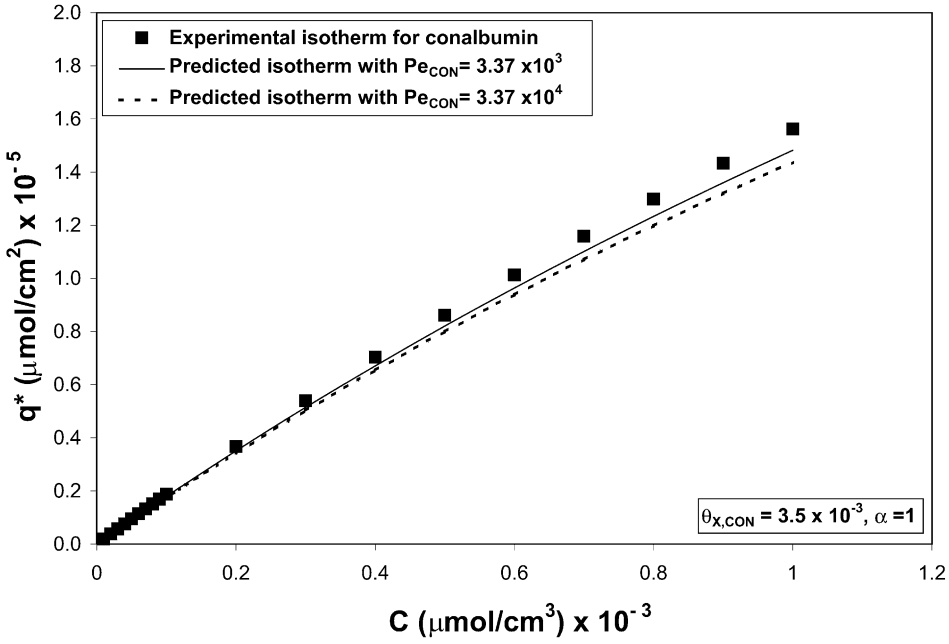


Fig. 4. Effect of *Pe* on prediction of linear isotherm region with the μOPPS.

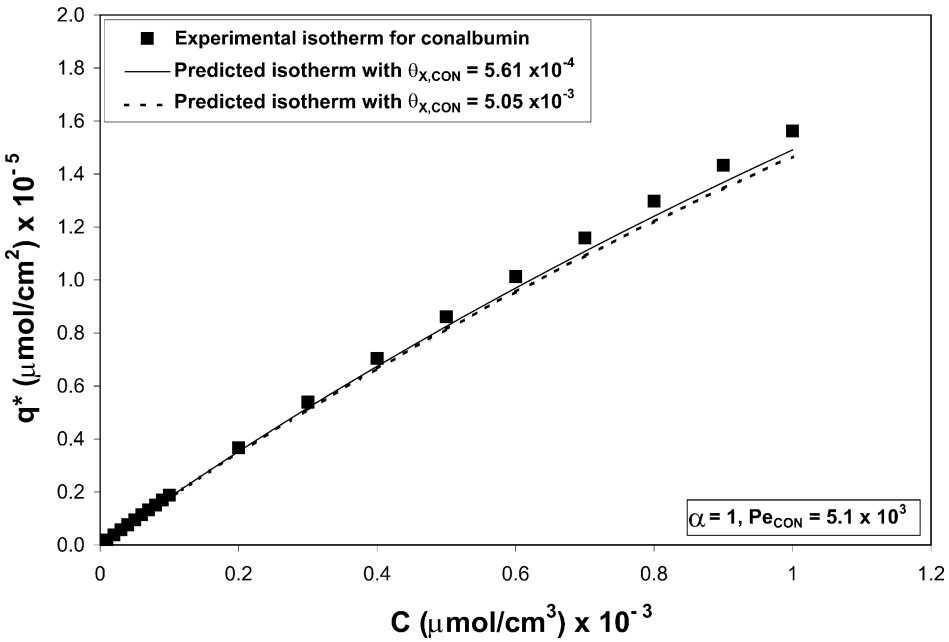


Fig. 5. Effect of $\theta_X$ on prediction of linear isotherm region with the μOPPS.

sorption is taking place only on the side-walls of the microchannel. $\theta_X$ is a sensitive measure of the effect of channel width. Fig. 5 shows that the accuracy of the HRM predictions increases as $\theta_X$ decreases. The deviations obtained in predicting $a_i$ range from 4 to 5% for conalbumin. It should be noted that the change in the accuracy of the prediction is small, despite a change in $\theta_X$ of an order of magnitude. This is because the range of widths used in the simulations ($b$ = 10–30 μm), as is typical in μOPPS, represents very narrow and therefore efficient channels.

For the μOPPS, the channel depth/width ratio ($\alpha$) can also affect performance. It has been shown earlier [21] that mass-transfer efficiency is dependent on α. Fig. 6 shows that the deviations increase with an increase in α. At $\alpha = 1$ deviations are approximately 5% for conalbumin, while at $\alpha = 100$ the deviations increase to 14%. Clearly, a square cross-section is most appropriate for evaluating the linear isotherm coefficient in a μOPPS.

Similar analyses were carried out for the μOTS. Figs. 7 and 8 show the results for the effects of *Pe* and $\theta_R$, re-

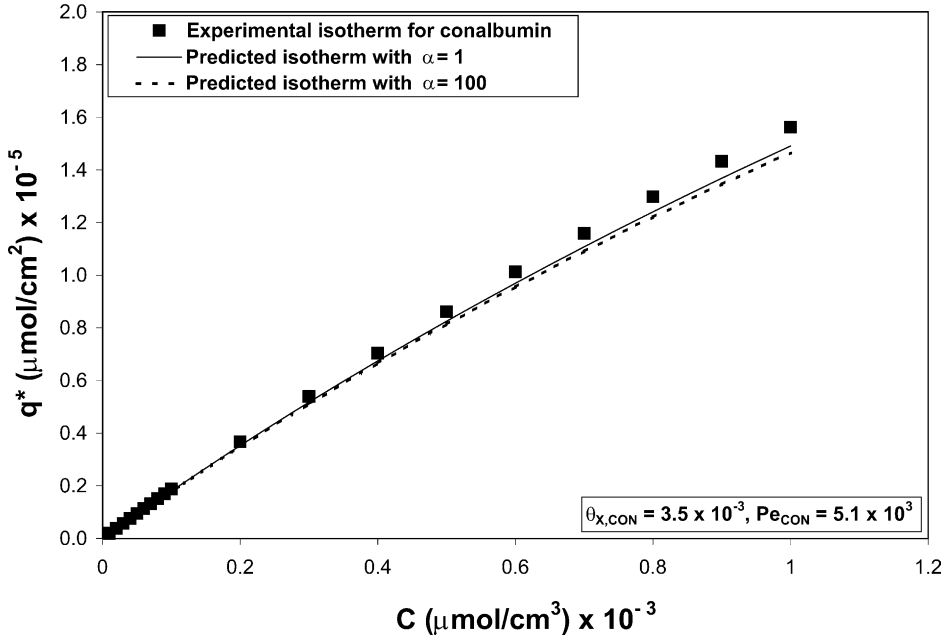


Fig. 6. Effect of $\alpha$ on prediction of linear isotherm region with the μOPPS.

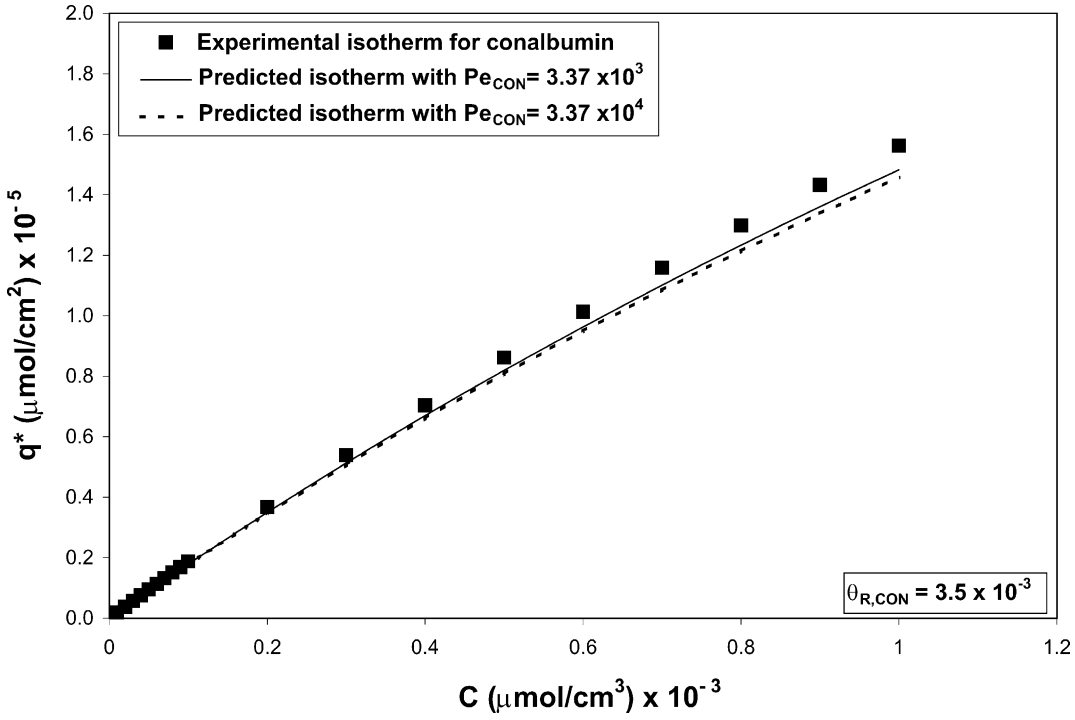


Fig. 7. Effect of *Pe* on prediction of linear isotherm region with the μOTS.

spectively. The results are similar to the μOPPS; i.e., the deviations increase with increasing *Pe* and increasing $\theta_R$. However, the deviations are generally smaller with the μOTS. In the μOPPS, liquid in the corners of the rectangular cross-section is almost stagnant. This is suspected to be the reason for the slightly larger deviations in the μOPPS. However, it is to be noted that the differences between isotherm predictions of the μOPPS and μOTS are

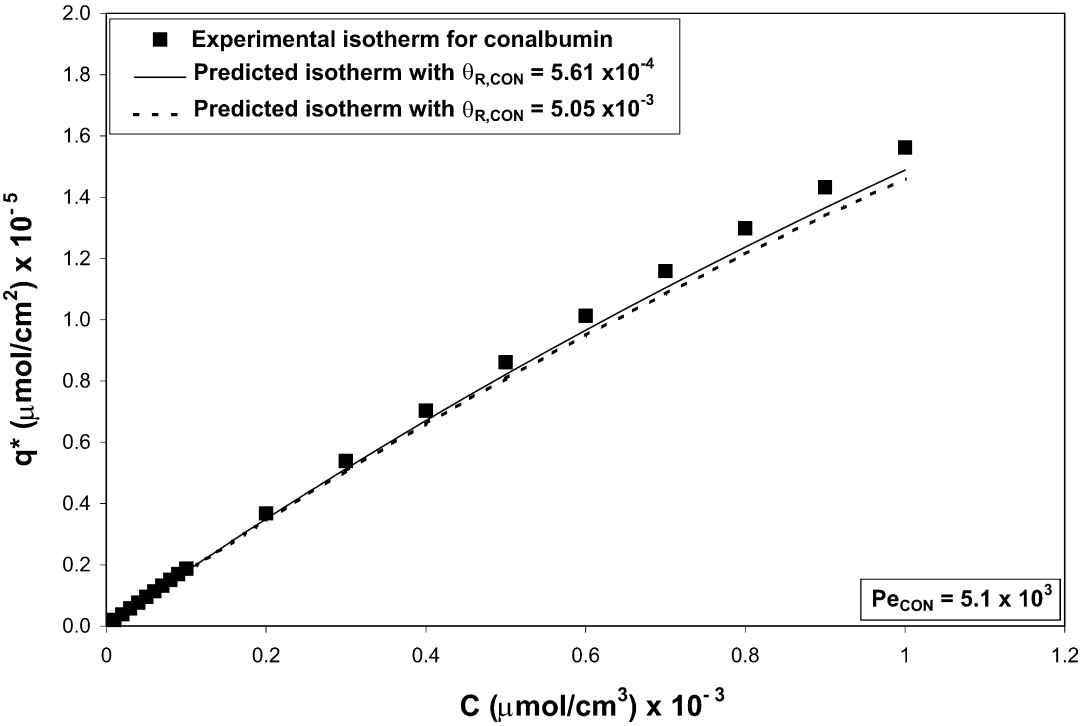


Fig. 8. Effect of $\theta_R$ on prediction of linear isotherm region with the μOTS.

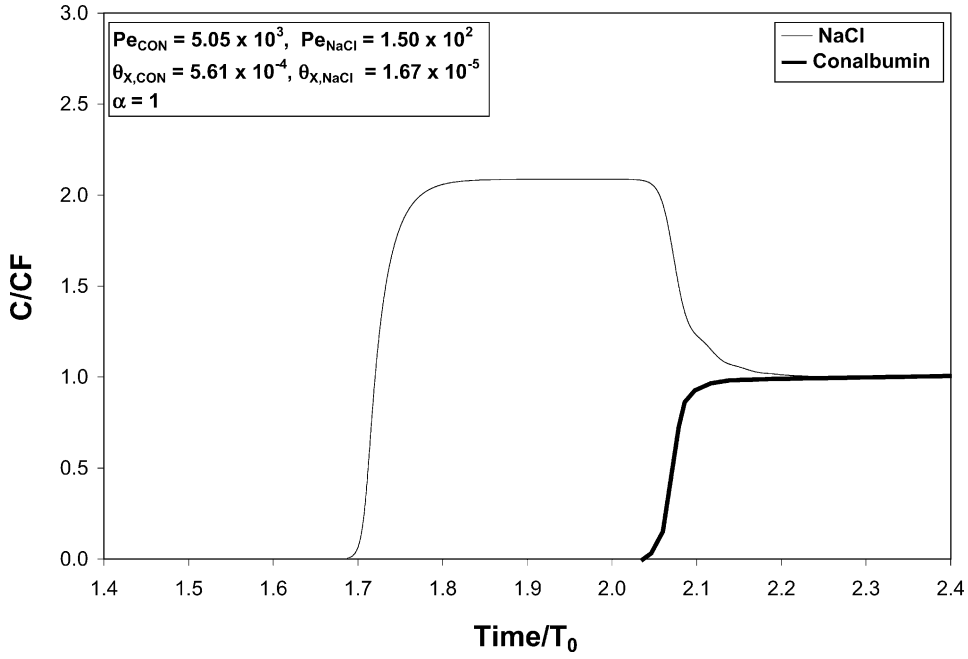


Fig. 9. Typical simulation results for non-linear frontal elution.

small, and both systems are suitable for use with HRM. One significant practical consideration is that the μOPPS is suitable for parallelization on a single chip, which has not been achieved with the μOTS [20]. This offers the possibility of carrying out multiple experiments simultaneously; for example, evaluating different adsorbent surface chemistries in parallel. This advantage may justify the small loss in estimation accuracy.

### *4.2. Prediction of the isotherm interference coefficients ($K_{m_i}$)*

The determination of the interference coefficient of the protein ($K_{m_i}$) by HRM requires a frontal injection of the protein at the salt concentration of interest. Further, to evaluate the effect of salt on this coefficient, frontal profiles must be obtained at a suitable number of salt concentrations in

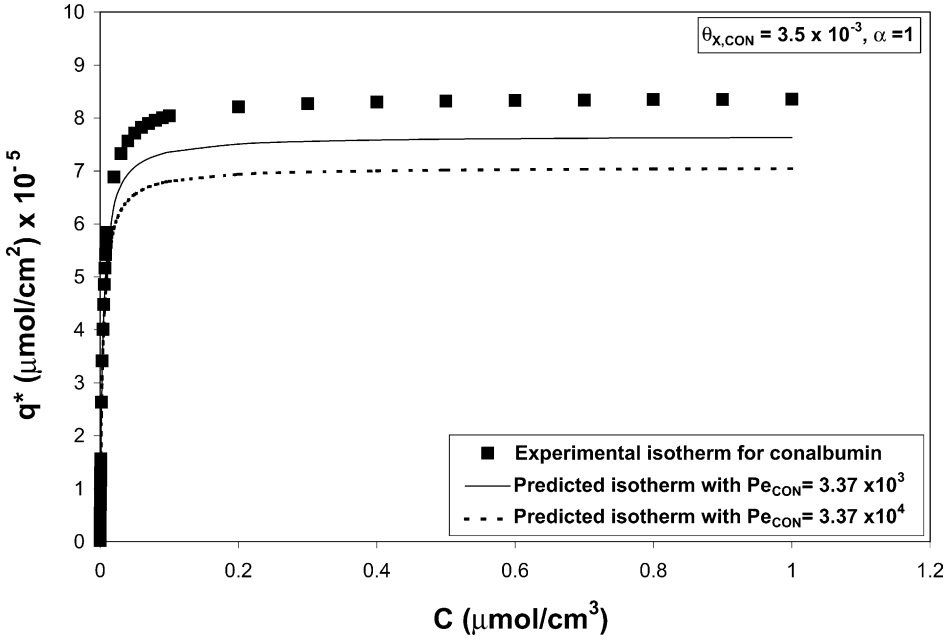


Fig. 10. Effect of *Pe* on prediction of non-linear isotherm region with the μOPPS.

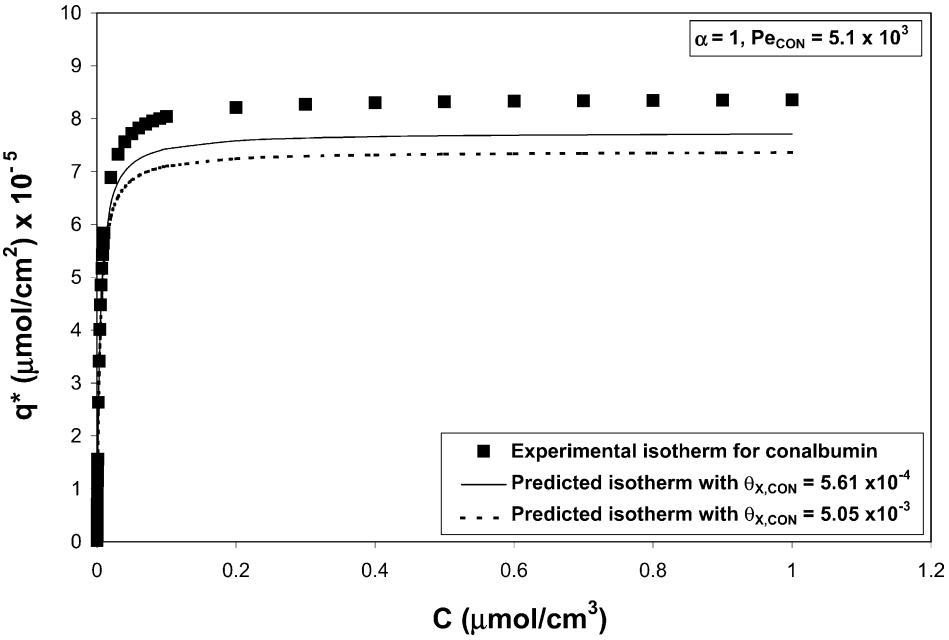


Fig. 11. Effect of $\theta_X$ on prediction of non-linear isotherm region with the μOPPS.

the range of interest. It is known that the prediction of $K_{m_i}$ is strongly dependent on band spreading [1], since it affects the accuracy with which the breakthrough times ($T_{RF}$) can be determined. Consequently, operating conditions must be carefully selected to minimize band spreading.

The effects of band spreading in the open-channel columns were evaluated using frontal simulations of protein–salt mixtures. A typical frontal development is shown in Fig. 9. Fig. 10 shows the influence of *Pe* on the prediction of $K_{m\mathrm{CON}}$ with a μOPPS. As with the estimation of the linear coefficient, deviations increase with increasing *Pe*. An increase of an order of magnitude in *Pe* increases the deviation in $K_{m\mathrm{CON}}$ from −5 to −11%. The estimation of the interference coefficient is sufficiently sensitive to *Pe*, that the liquid velocity and channel length must be carefully selected to match the diffusion coefficient of the protein.

Figs. 11 and 12 show the dependence of the predictions of $K_{m\mathrm{CON}}$ on $\theta_X$ and $\alpha$, respectively. The deviations in $K_{m\mathrm{CON}}$ go from −4 to −8%, as $\theta_X$ changes over an order of magnitude. This indicates that the channel widths in μOPPS are

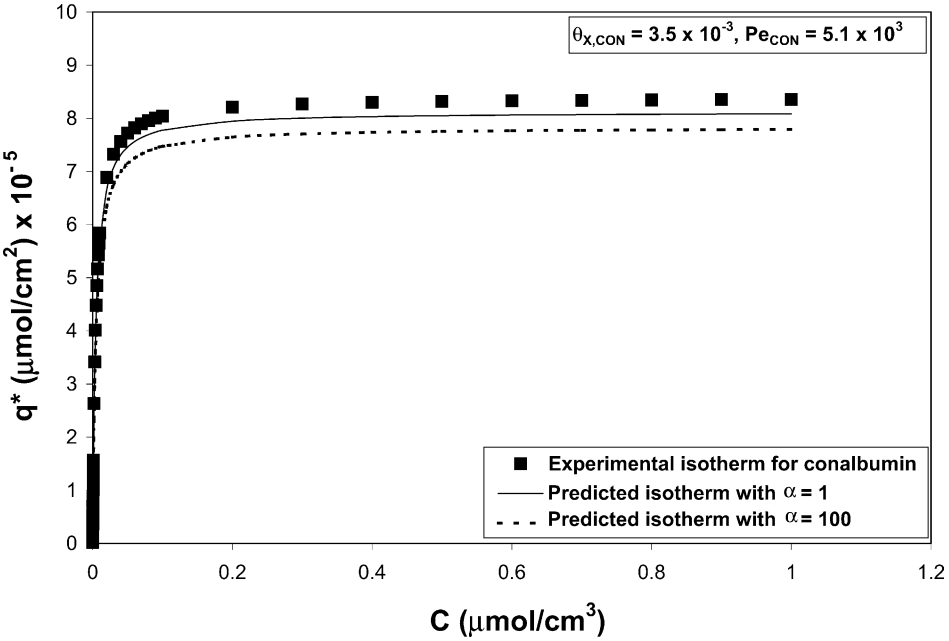


Fig. 12. Effect of $\alpha$ on prediction of non-linear isotherm region with the μOPPS.

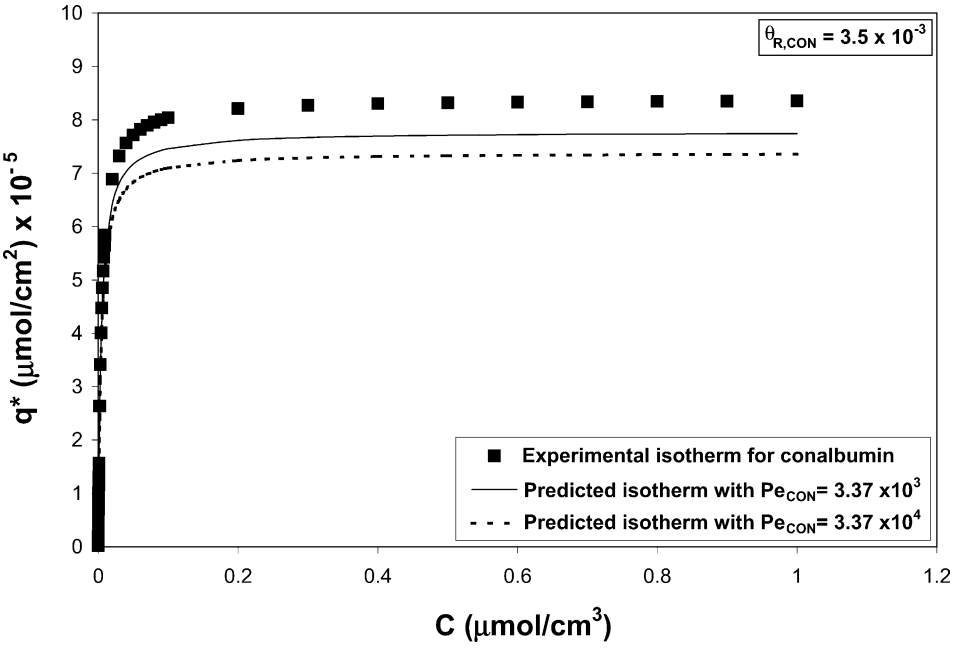


Fig. 13. Effect of *Pe* on prediction of non-linear isotherm region with the μOTS.

well suited for rapid mass transfer of the proteins to the wall, as is assumed by HRM. By comparing the results in Figs. 10 and 11 it can be observed that the μOPPS is more sensitive to an order of magnitude change in *Pe* than to a similar change in $\theta_X$.

The results in Fig. 12 show deviations from −6 to 12% as $\alpha$ is increased from 1 to 100. Increasing $\alpha$ increases the characteristic length for diffusion along the depth of the channel, and as a result larger concentration gradients form along the width and depth [21]. Thus, for the estimation of both the linear and interference coefficients, a μOPPS with a square cross-section is best.

Figs. 13 and 14 show the results obtained in the μOTS as a function of *Pe* and $\theta_R$, respectively. These are similar to those obtained with the μOPPS; increasing *Pe* or $\theta_R$ increases the deviation in the predictions of the Langmuir parameters, and the μOTS is more sensitive to changes in *Pe* than to changes in $\theta_R$. As with the linear elution simulations, the deviations in predicting $K_{m_i}$ obtained with the μOTS are slightly smaller than those obtained with the μOPPS. This

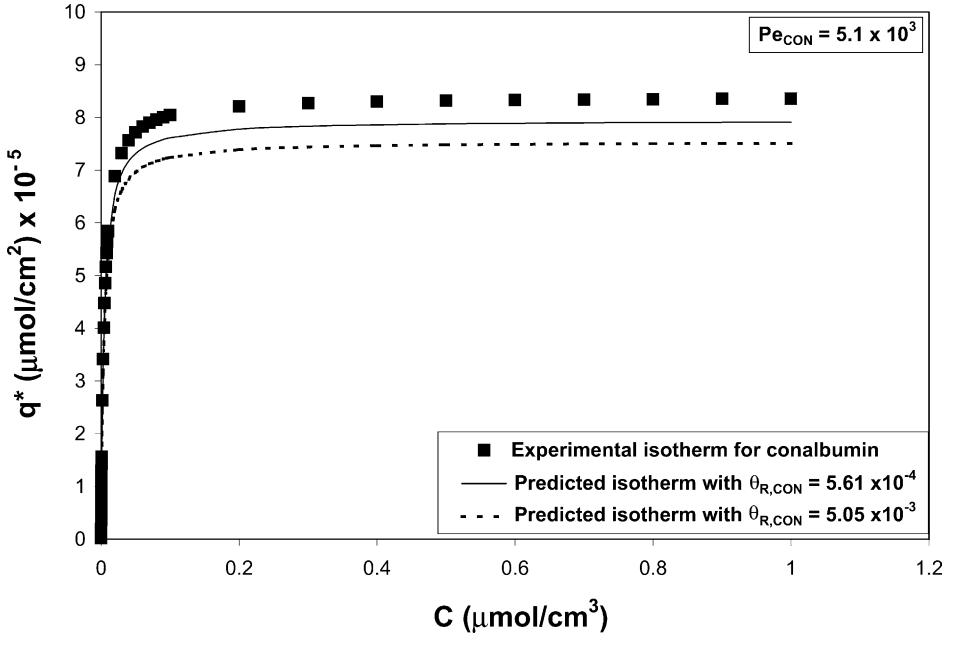


Fig. 14. Effect of $\theta_R$ on prediction of non-linear isotherm region with the μOTS.

is due to the smooth perimeter of flow in the μOTS, as was discussed earlier.

For both the μOPPS and μOTS, it is observed that the estimated non-linear isotherm always falls below the experimental value (Figs. 10–14). This is a consequence of the influence of mass transfer on the frontal breakthrough time. Dispersive effects reduce the frontal breakthrough time relative to that under equilibrium conditions. This results in an overestimate of $K_m$ and an underestimate of capacity. For protein–salt systems, to ensure an accurate estimation of $K_m$, it is recommended that the fluid velocity ($v_{avg}$) and the channel length ($L$) be selected to give a *Pe* of $10^3$ or less.

## 5. Conclusions

The H-root method has been adapted for the evaluation of adsorption isotherms in μOPPS and μOTS chromatographic systems. HRM utilizes chromatographic responses to predict the Langmuir coefficients of the analytes. The results show that for both open micro-channel systems, by selecting the appropriate operating and geometrical conditions, it is possible to obtain accurate protein adsorption isotherms in the presence of salt, for systems that give a Type I (Langmuir) isotherm. This is primarily attributed to efficient mass transfer of the protein to the surface due to the short characteristic length for diffusion. This ensures close correspondence to the assumption of HRM. In general, the μOTS gave more accurate predictions of the isotherm coefficients than the μOPPS in both linear and overloaded regions. This is postulated to be due to the absence of dead zones in the flow cross-section.

## 6. Nomenclature

### 6.1. Symbols

| | |
|---|---|
| $a$ | Langmuir affinity coefficient (linear isotherm coefficient) (cm) |
| $b$ | microchannel half width (cm) |
| $C$ | solute concentration in the mobile phase (μmol/cm$^3$) |
| CF | feed concentration (μmol/cm$^3$) |
| $d$ | microchannel half depth (cm) |
| $D$ | diffusion coefficient in solution (cm$^2$/s) |
| $k$ | linear elution column capacity factor (dimensionless) |
| $K$ | frontal capacity factor (dimensionless) |
| $K_m$ | Langmuir competitive interference coefficient (cm$^3$/μmol) |
| $L$ | microchannel length (cm) |
| *Pe* | Peclet number (dimensionless), $Pe_i = (v_{avg} L/D_i)$ |
| $q^*$ | equilibrium concentration of solute in the stationary phase (μmol/cm$^2$) |
| $r_C$ | μOTS radius (cm) |
| $R$ | dimensionless position along the μOTS radius |
| $t$ | time (s) |
| $T_0$ | holdup time (s) |
| $T_R$ | retention time (s) |
| $T_{RF}$ | frontal breakthrough time (s) |
| $v_{avg}$ | average linear velocity along the length (cm/s) |
| VC | column volume (cm$^3$) |
| $v_C$ | concentration velocity (cm/s) |
| VF | feed volume (cm$^3$) |
| $V_m$ | Langmuir parameter (μmol/cm$^2$) |
| $v_y$ | linear velocity along the length (cm/s) |
| $x$ | position along the microchannel width (cm) |
| $X$ | dimensionless position along the microchannel width, $X = (x/b)$ |
| $y$ | position along the microchannel length (cm) |
| $Y$ | dimensionless position along the microchannel length, $Y = (y/L)$ |
| $z$ | position along the microchannel depth (cm) |
| $Z$ | dimensionless position along the microchannel depth, $Z = (z/d)$ |

### 6.2. Greek symbols

| | |
|---|---|
| $\alpha$ | $\theta_Z/\theta_X$ ratio (dimensionless) |
| $\phi$ | phase ratio (cm$^{-1}$) |
| $\theta_R$ | dimensionless time, $\theta_{R,i} = (v_{avg} r_C^2/D_i L)$ |
| $\theta_X$ | dimensionless time, $\theta_{X,i} = (v_{avg} b^2/D_i L)$ |
| $\theta_z$ | dimensionless time, $\theta_{Z,i} = (v_{avg} d^2/D_i L)$ |
| $\tau$ | dimensionless time, $\tau = (v_{avg} t/L)$ |

## References


[1] T. Chen, N.G. Pinto, L.V. Brocklin, J. Chromatogr. 484 (1989) 167.
[2] T.W. Hearn, in: C.T. Mant, R.S. Hodges (Eds.), High Performance Liquid Chromatography of Peptides and Proteins, CRC Press, Boca Raton, FL, 1991, p. 95.
[3] M. Thrash, N.G. Pinto, in A. Holyoak, (Ed.), Protein and Peptides Purification in Pharmaceutical Analysis, in: Encyclopedia of Analytical Chemistry, Wiley, Chichester, 2000, pp. 7259–7288.
[4] M.R. Ladisch, Bioseparations Engineering: Principles, Practice and Economics, Wiley–Interscience, New York, 2001.
[5] A. Felinger, G. Guiochon, J. Chromatogr. A 724 (1996) 27.
[6] J.M. Jacobson, J.H. Frenz, C. Horváth, Ind. Eng. Chem. Res. 26 (1987) 43.
[7] F. James, M. Sepúlveda, F. Charton, I. Quiñones, G. Guiochon, Chem. Eng. Sci. 54 (1999) 1677.
[8] O. Lisec, P. Hugo, A. Seidel-Morgenstern, J. Chromatogr. A 908 (2001) 19.
[9] F. Gritti, G. Gotmar, B.J. Stanley, G. Guiochon, J. Chromatogr. A 988 (2003) 185.
[10] A. Felinger, D. Zhou, G. Guiochon, J. Chromatogr. A 1005 (2003) 35.
[11] S.C.D. Jen, N.G. Pinto, J. Chromatogr. A 662 (1994) 396.
[12] H.W. Yu, Y.X. Wu, C.B. Ching, Chromatographia 57 (2003) 161.
[13] J. Newburger, B. Delange, G. Guiochon, J. Chromatogr. A 684 (1994) 1.
[14] F. Helfferich, G. Klein, Multicomponent Chromatography: Theory of Interference, Marcel Dekker, New York, 1970.

[15] F.G. Helfferich, R.D. Whitley, J. Chromatogr. A 734 (1996) 7.
[16] F.G. Helfferich, Chem. Eng. Sci. 46 (1991) 3320.
[17] G. Guiochon, S. Golshan-Shirazi, A.M. Katti, Fundamentals of Preparative and Non-linear Chromatography, Academic Press, Boston, MA, 1994.
[18] F.G. Helfferich, J. Chromatogr. A 768 (1997) 169.
[19] G.E. Spangler, Anal. Chem. 70 (1998) 4805.
[20] Q. Kang, N.C. Golubovic, N.G. Pinto, H.T. Henderson, Chem. Eng. Sci. 56 (2001) 3409.
[21] B.H. Lapizco-Encinas, N.G. Pinto, Sep. Sci. Technol. 37 (2002) 2745.
[22] B.H. Lapizco-Encinas, Ph.D. Dissertation, University of Cincinnati, Cincinnati, 2003.
[23] M.T. Tyn, T.W. Gusek, Biotechnol. Bioeng. 35 (1990) 327.
[24] A. Chandavarkar, N.G. Pinto, Fundam. Adsorpt. 6 (1998) 413.